Article

Current Biology

Mechanochemical feedback mediates tissue bending required for seedling emergence

Graphical Abstract

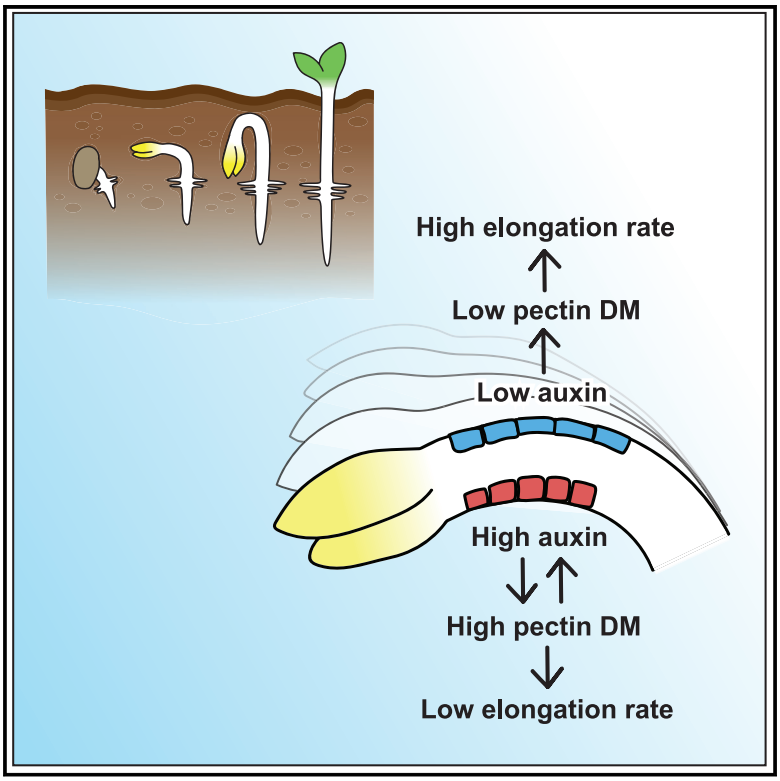

Highlights

- Asymmetric pectin methylesterification is required for differential growth
- Auxin distribution regulates pectin methylesterification during differential growth
- Feedback between pectin and auxin via PIN proteins facilitates growth asymmetry

Authors

Kristoffer Jonsson, Rahul S. Lathe, Daniel Kierzkowski, Anne-Lise Routier-Kierzkowska, Olivier Hamant, Rishikesh P. Bhalerao

Correspondence

kristoffer.jonsson@slu.se (K.J.), rishi.bhalerao@slu.se (R.P.B.)

In Brief

Using hook development as model in *Arabidopsis*, Jonsson et al. demonstrate a mechanochemical feedback between the plant hormone auxin and pectin methylesterification regulates differential cell elongation to facilitate tissue bending essential for seedling emergence from soil.

Jonsson et al., 2021, Current Biology *31*, 1154–1164
March 22, 2021
https://doi.org/10.1016/j.cub.2020.12.016

CellPress

CellPress
OPEN ACCESS

Current Biology

Article

Mechanochemical feedback mediates tissue bending required for seedling emergence

Kristoffer Jonsson,[1,4,5,*] Rahul S. Lathe,[1,4] Daniel Kierzkowski,[2] Anne-Lise Routier-Kierzkowska,[2] Olivier Hamant,[3] and Rishikesh P. Bhalerao[1,5,6,*]

[1]Umeå Plant Science Centre, Department of Forest Genetics and Plant Physiology, Swedish University of Agricultural Sciences, 90187 Umeå, Sweden
[2]IRBV, Department of Biological Sciences, University of Montreal, 4101 Sherbrooke Est, Montréal H1X 2B2, QC, Canada
[3]Laboratoire Reproduction et Développement des Plantes, Univ Lyon, ENS de Lyon, UCB Lyon 1, CNRS, INRA, Lyon, France
[4]These authors contributed equally
[5]Senior author
[6]Lead contact
*Correspondence: kristoffer.jonsson@slu.se (K.J.), rishi.bhalerao@slu.se (R.P.B.)
https://doi.org/10.1016/j.cub.2020.12.016

SUMMARY

Tissue bending is vital to plant development, as exemplified by apical hook formation during seedling emergence by bending of the hypocotyl. How tissue bending is coordinated during development remains poorly understood, especially in plants where cells are attached via rigid cell walls. Asymmetric distribution of the plant hormone auxin underlies differential cell elongation during apical hook formation. Yet the underlying mechanism remains unclear. Here, we demonstrate spatial correlation between asymmetric auxin distribution, methylesterified homogalacturonan (HG) pectin, and mechanical properties of the epidermal layer of the hypocotyl in *Arabidopsis*. Genetic and cell biological approaches show that this mechanochemical asymmetry is essential for differential cell elongation. We show that asymmetric auxin distribution underlies differential HG methylesterification, and conversely changes in HG methylesterification impact the auxin response domain. Our results suggest that a positive feedback loop between auxin distribution and HG methylesterification underpins asymmetric cell wall mechanochemical properties to promote tissue bending and seedling emergence.

INTRODUCTION

During seedling emergence, differential growth causes the hypocotyl to bend into an apical hook, which protects the fragile shoot apical meristem from the soil interface. Hook formation relies primarily on asymmetric cell elongation on two sides of the young hypocotyl, leading to bending of this organ.[1]

The regulation of growth asymmetry, which culminates in a 180° bend, is coordinated by an intrinsic system dominated by the hormone indole-3-acetic acid (IAA/auxin).[2] Experiments using the synthetic auxin reporter DR5 have revealed that the transcriptional auxin response is primarily localized to the inner side of the hook.[3] Auxin is both a promoter and inhibitor of cell elongation depending on the organ.[4] In the *Arabidopsis* apical hook, high auxin levels on the inner side are associated with a reduction in cell elongation relative to the outer side,[5,6] resulting in bending of the hypocotyl. Previous studies in which genetic interference with auxin metabolism, transport, or signaling caused severe apical hook defects further support a critical role of auxin in hook development.[6–8] However, the mechanical aspects of cell growth have not been integrated with auxin distribution, and the rapid bending of the hook suggests the existence of an amplification mechanism, which also remains elusive.

Plant cells are enclosed within a rigid cell wall—cell elongation is only possible if the cell wall yields to turgor.[9] Thus, cell wall remodeling is at the nexus between auxin activity and tissue bending. In agreement, the promoting effect of auxin on cell elongation described in great detail is thought to involve increased wall extensibility through acidification of the wall and activation of cell wall-loosening proteins as well as through transcriptional control of cell wall-modifying enzymes.[10,11] In particular, auxin triggers the de-methylesterification of pectin, resulting in wall softening and organ emergence, at the shoot apical meristem in *Arabidopsis*.[12] In contrast, the downstream events associated with auxin-induced inhibition of cell growth, notably in the root, are less well understood but could involve wall alkalinisation.[13] Whether this involves pectin modifications is unknown.

The pectic polysaccharide homogalacturonans (HGs) are a major constituent of the cell wall in expanding cells.[14] Synthesized in the Golgi,[15] HGs are delivered to the wall with a high degree of methylesterification.[16] HGs are selectively de-methylesterified through the action of pectin methylesterases (PMEs), which are inhibited by PME inhibitors (PMEIs).[17] Previous studies have demonstrated that HG de-methylesterification can enhance cell wall softening, extensibility, and expansion.[18,19] Although debated,[20] there is evidence from elongating hypocotyls that the loosening of longitudinal walls, which precedes anistropic growth, depends on the level of HG methylesterification, with a high degree of HG methylesterification stiffening the

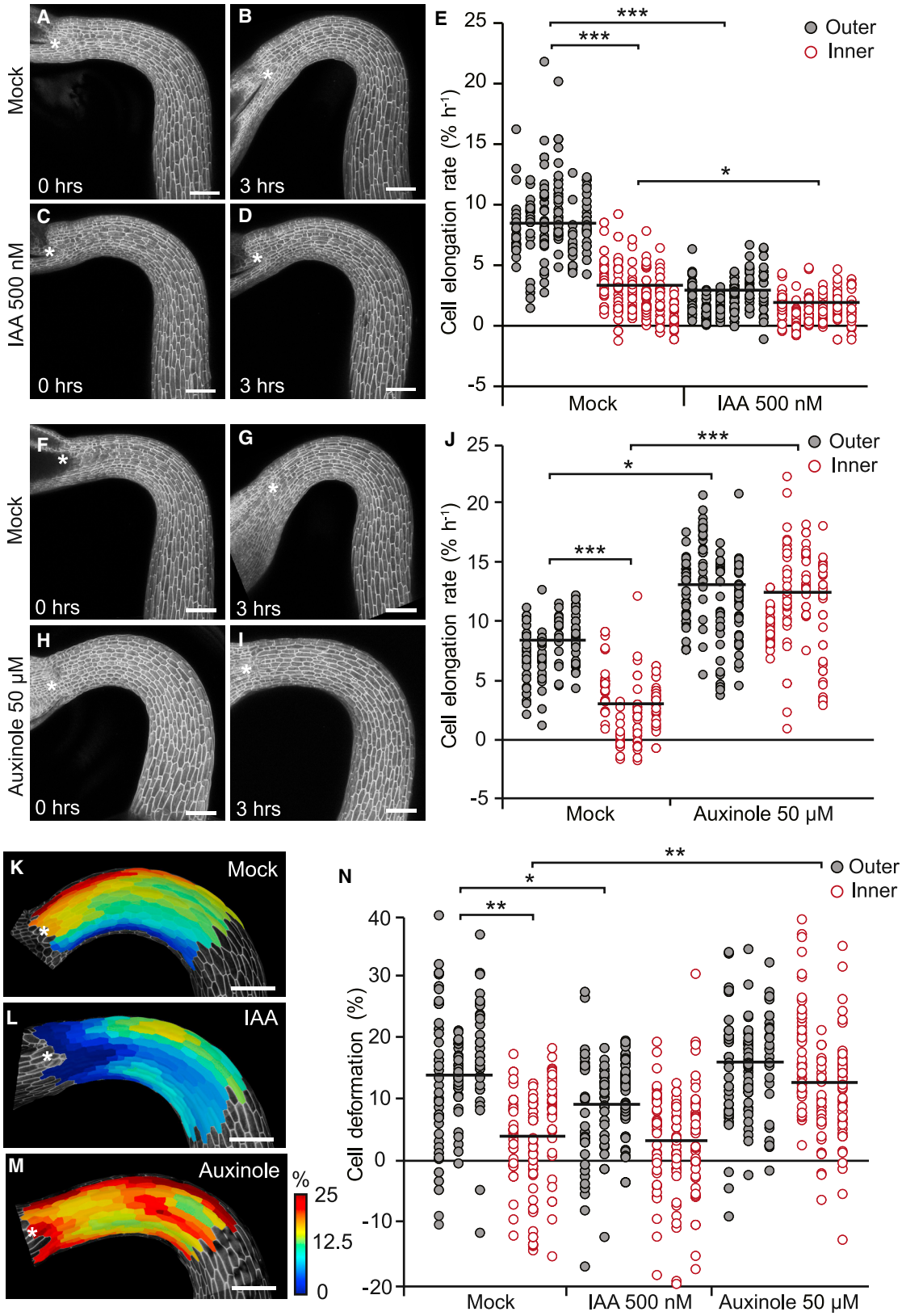

(legend on next page)

cell walls.[19] Consistently, primordium initiation in the apical meristem is preceded by auxin-induced wall loosening through HG de-esterification, with ectopic PMEI expression inhibiting primordia development.[21]

Previous findings that the regulation of HG methylesterification is crucial to modifying cell mechanical properties for growth asymmetry at both the cell and tissue level prompted us to study the interplay between HG methylesterification, cell wall mechanics, and auxin in hook development. Our results reveal that a positive feedback loop between HG methylesterification and auxin mediates and amplifies differential cell elongation for tissue bending during hook development.

RESULTS

Auxin modulates cell elongation and mechanical properties

Tissue bending during apical hook development is a result of differential cell elongation on two sides of the hypocotyl.[22,23] Genetic analyses have shown that auxin plays a key role in hook development.[6,24] Moreover, auxin response in the apical hook is asymmetric and inversely correlated with cell elongation.[5] In particular, using auxin transport mutants, it has been suggested that the strong auxin response on the inner side reduces cell elongation relative to the outer side and partly explains hypocotyl bending.[6] Here, we addressed the role of auxin distribution and its interaction with the cell wall to understand tissue bending during hook development.

First, we examined the effect of auxin on cell elongation in the hypocotyl of dark grown *Arabidopsis* seedlings, focusing on the region at 0–400 μm from the shoot apical meristem (SAM), where elongation asymmetry was highly pronounced in Col-0 wild-type (WT) (Figure S1; $n \geq 18$ cells from each of 6 seedlings), as shown previously.[22] Exogenous IAA application to WT seedlings for 3 h during hook formation strongly reduced cell elongation rates relative to mock-treated WT seedlings (Figures 1A–1E; $n \geq 25$ cells from each of 6 seedlings). The most pronounced effect was observed on the outer side, i.e., a 3-fold reduction in the cell elongation rates upon IAA treatment relative to mock (2.4% h^{-1} ± 0.8% in IAA-treated cells, compared to 8.2% h^{-1} ± 1.6% in mock-treated cells), while elongation in cells on the inner side reduced from 2.6% h^{-1} ± 1.0% upon mock to 1.4% h^{-1} ± 0.5% upon IAA treatment. Conversely, inhibiting auxin response by exogenously applying the auxin antagonist auxinole for 3 h, cell elongation rate was increased 3-fold on the inner side compared with mock treatment (on the inner side, 11.7% h^{-1} ± 2.2% upon auxinole treatment compared to 2.9% h^{-1} ± 1.7% upon mock treatment), while auxinole only mildly enhanced elongation on the outer side (12.6% h^{-1} ± 2.0% upon auxinole treatment compared to 8.0% h^{-1} ± 1.1% upon mock treatment) (Figures 1F–1J; $n \geq 16$ cells from each of 4 seedlings). Taken together, these results formally demonstrate that auxin reduces cell elongation rates during hook formation.

Cell elongation rates correlate with mechanical properties in the apical hook,[22] and, since auxin reduces cell elongation during hook formation as shown above, we investigated the impact of auxin on the mechanical properties of cell walls. We used a previously described approach of modulating turgor pressure by osmotic treatments and measuring elastic cell deformation to gain further insight into cell wall mechanical properties. This approach has been used to analyze mechanical properties of cell wall. This notably revealed that cell wall stiffness[25] correlates with cellular growth patterns in various tissues.[22,26] To assess the impact of auxin on wall mechanical properties, we performed cell deformation assays following exogenous application of auxin and auxinole. In agreement with previous data, there was a significant difference in cell deformation between the inner and outer side of the hook in the region at 0–400 μm from SAM. Exogenous addition of auxin for 3 h resulted in significantly reduced cell deformation mainly on the outer side (9.3% ± 2.2% upon IAA compared with 14.0% ± 3.1% upon mock treatment) while the inner side was not affected by IAA treatment (3.2% ± 2.6% upon IAA treatment compared with 3.9% ± 3.1% upon mock treatment) (Figures 1K–1L and 1N; $n \geq 13$ cells from each of 3 seedlings). In contrast, suppressing the auxin response through auxinole application for 3 h increased cell deformation on the inner side of the hook 3-fold relative to the control (12.0% ± 4.3% upon auxinole treatment compared with 3.9% ± 3.1% upon mock treatment), while auxinole treatment had little effect on the outer side (15.7% ± 1.7% upon auxinole compared with 14.0% ± 3.1% upon mock treatment) (Figures 1M and 1N; $n \geq 13$ cells from each of 3 seedlings). These results suggest that asymmetric auxin distribution could mediate differential cell elongation, with high auxin levels promoting wall stiffness and reducing cell elongation on the inner side.

Differential HG methylesterification is required for hook development and seedling emergence

Cell wall mechanical properties are determined by cell wall composition and texture.[9] However, the wall components that could mediate mechanical asymmetry during hook development are not well known. Several recent studies have demonstrated that HG methylesterification levels affect cell wall mechanical properties in the SAM and in the hypocotyl.[18,19] We therefore

Figure 1. Auxin modulates cell elongation and mechanical properties during hook formation

(A–D) Time-lapse images of cells in WT during formation upon mock (A and B) or IAA 500 nM (C and D).

(E) Individual cell-elongation rates (% h^{-1}) at 0–400 μm from SAM upon 3 h mock and 500 nM IAA treatment. $n \geq 25$ cells from each of 6 seedlings. Cells from individual seedlings are grouped vertically. Black horizontal lines indicate the mean.

(F–I) Time-lapse images of seedlings during formation upon mock (F and G) or auxinole 50 μM (H and I).

(J) Individual cell-elongation rates (% h^{-1}) at 0–400 μm upon 3 h mock and 50 μM auxinole treatment. $n \geq 16$ cells from each of 4 seedlings. Cells from individual seedlings are grouped vertically. Black horizontal lines indicate the mean.

(K–M) Heatmaps of cell deformation upon 3 h mock (K), 3 h 500 nM IAA (L), or 50 μM auxinole treatment (M).

(N) Percent cell deformation upon 3 h mock, 3 h 500 nM IAA, or 3 h 50 μM auxinole treatment. $n \geq 13$ cells from each of 3 seedlings. Cells from individual seedlings are grouped vertically. Black horizontal lines indicate the mean.

Statistical significance was determined by paired, two-tailed Student's t test, where $^{*}p < 0.05$, $^{**}p < 0.005$, $^{***}p < 0.0005$. Error bars represent standard deviation of the mean. White asterisks in (A)–(D), (F)–(I), and (K)–(M) mark position of SAM. All scale bars 100 μm. See also Figure S1.

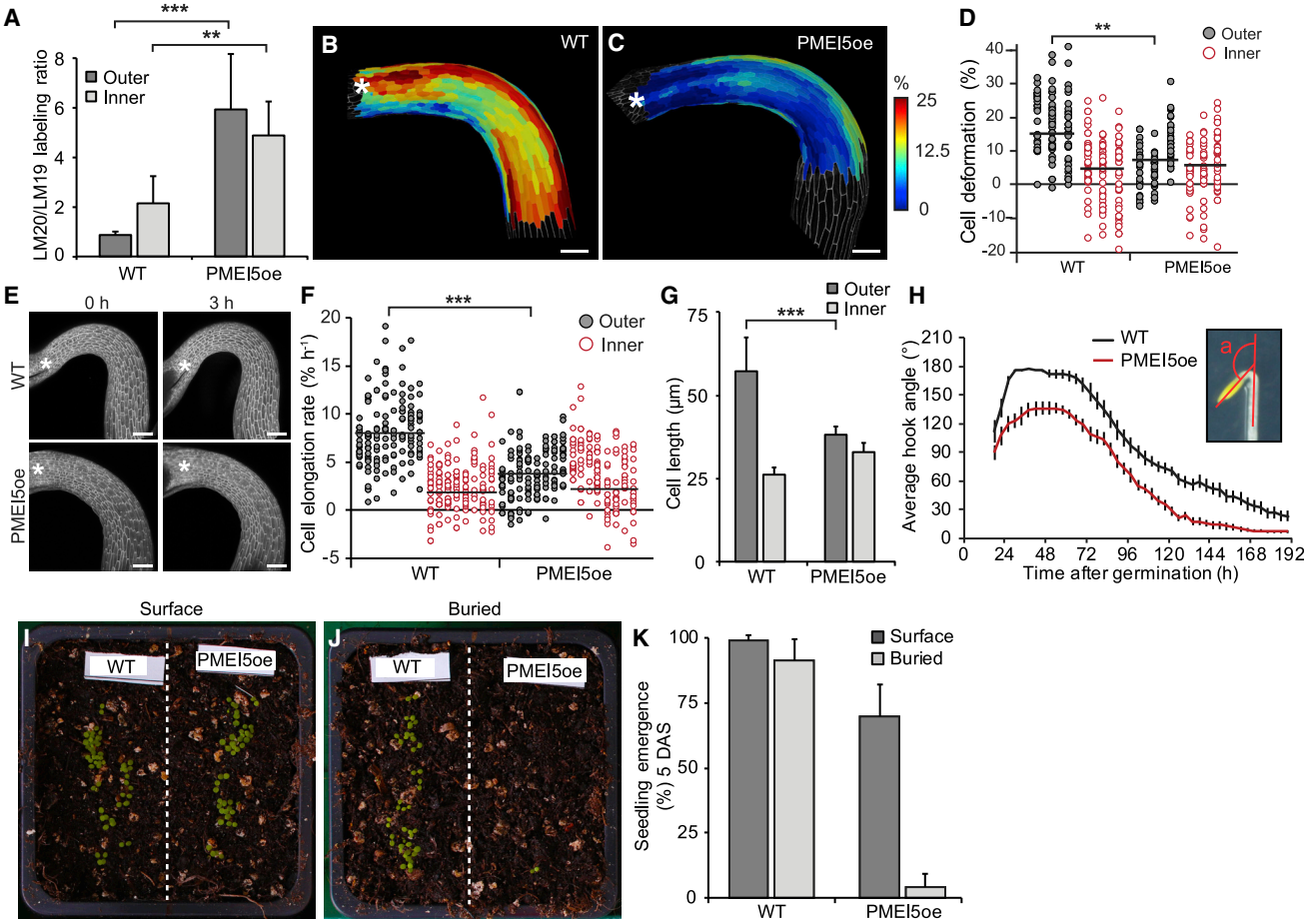

Figure 2. Asymmetric HG methylesterification is required for proper hook development

(A) Ratio of LM20 and LM19 labeling fluorescence intensity for longitudinal walls of individual epidermal cells in WT and PMEI5oe seedlings at 0–400 μm from SAM. n ≥ 11 cells from each of 8 seedlings.

(B and C) Heatmaps of cell deformation in WT (B) and PMEI5oe (C).

(D) Percentage of cell deformation at 0–400 μm from SAM in WT and PMEI5oe. n ≥ 14 cells from each of 3 seedlings. Cells from individual seedlings are grouped vertically. Black horizontal lines indicate the mean.

(E), Macro-confocal time-lapse images of cells in WT and PMEI5oe at 0 and 3 h during formation.

(F) Cell-elongation rates of epidermal cells at 0–400 μm from SAM in WT and PMEI5oe seedlings during formation. n ≥ 13 cells from each of 8 seedlings. Cells from individual seedlings are grouped vertically. Black horizontal lines indicate the mean.

(G) Cell lengths of epidermal cells in WT and PMEI5oe seedlings at early hook maintenance phase, 30 h after germination. n ≥ 80 cells from each of 6 seedlings.

(H) Apical hook development in WT and PMEI5oe seedlings. n = 16 seedlings. Inset depicts hook angle was obtained.

(I and J) Seedling emergence when germinated on the soil surface (I) or buried 5 mm into soil (J).

(K) Quantification of soil emergence based on (I) and (J). n = 30 seeds, repeated 3 times.

In (A) and (K), error bars represent standard deviation of the mean. In (H), error bars represent standard error of the mean. Statistical significance was determined by paired, two-tailed Student's t test, where $^{**}p < 0.005$, $^{***}p < 0.0005$. White asterisks in (B), (C), and (E) mark the position of SAM. All scale bars, 100 μm. See also Figure S2.

examined the role of HG methylesterification in differential growth during apical hook development. To this end, we first investigated the spatial pattern of HG methylesterification between 0 and 400 μm from SAM, where elongation asymmetry and differences in cell-wall mechanical properties were most pronounced. We labeled cell walls of WT with the antibodies LM20 and LM19, which preferentially label highly methylesterified and de-methylesterified HG, respectively. At 0–400 μm from SAM, the LM20/LM19 labeling ratio of longitudinal epidermal walls was higher (over 2-fold) in cells on the inner side of the hook (labeling ratio 1.9 ± 1.0) than corresponding cells on the outer side (0.8 ± 0.1) (Figures 2A and S2A; n ≥ 11 cells per seedling, from 8 seedlings). Hence, epidermal cells close to the SAM—the region with the largest asymmetry in cell growth and cell wall mechanical properties—also displayed a pronounced spatial asymmetry in HG methylesterification levels with high HG methylesterification levels correlating with slower growing cells and the opposite trend on the outer side.

We next investigated whether asymmetric HG methylesterification is essential for hook development. We genetically

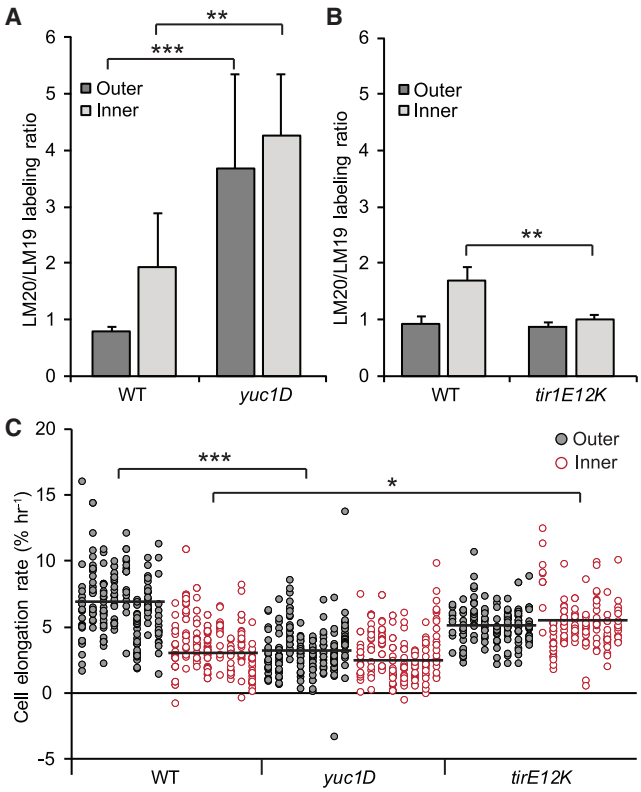

Figure 3. Auxin promotes HG methylesterification in the apical hook

(A and B) Quantification of immunolabeling intensity ratio of LM20 and LM19 in longitudinal walls of epidermal cells at 0–400 μm from SAM based on confocal images of 2.5 μm sections in WT and *yuc1D* (A) and WT and *tir1E12K* (B). For (A), n ≥ 10 cells from each of ≥6 seedlings, for (B), n ≥ 6 cells from each of 4 seedlings.

(C) Individual cell-elongation rates of epidermal cells at 0–400 μm from SAM in WT, *yuc1D*, and *tirE12K* seedlings during formation. n ≥ 10 cells from each of 8 seedlings. Cells from individual seedlings are grouped vertically. Black horizontal lines indicate the mean. Statistical significance was determined by paired, two-tailed Student's t test, where **p < 0.005, ***p < 0.0005. Error bars represent standard deviation of the mean. See also Figure S3.

perturbed HG methylesterification asymmetry by expressing PECTINMETHYLESTERASE INHIBITOR 5 (PMEI5oe).[27] Ectopic PMEI5 expression markedly elevated epidermal HG methylesterification levels relative to what was observed in WT cells at 0–400 μm from SAM (LM20/LM19 ratio in PMEI5oe: 4.4 ± 1.2 on inner side and 5.3 ± 2.0 on outer side compared with WT: 1.9 ± 1.0 on inner side and 0.8 ± 0.1 on outer side) (Figures 2A and S2A; n ≥ 11 cells from each of 8 seedlings); thus, asymmetric HG methylesterification was severely attenuated in PMEI5oe seedlings relative to WT seedlings. We also investigated cell wall mechanical properties in the PMEI5oe seedlings between 0 and 400 μm from SAM as evaluated for the WT hook. In comparison to WT seedlings, the PMEI5oe seedlings exhibited a severe reduction in cell deformation on the outer side (6.7% ± 6.5% in PMEI5oe compared with 15.0% ± 3.0% in WT) (Figures 2B–2D; n ≥ 14 cells from each of 3 seedlings). Correspondingly, we observed a strong reduction in cell elongation rates in PMEI5oe on the outer side (3.8% h^{-1} ± 1.2% in PMEI5oe compared with 8.1% h^{-1} ± 1.4% in WT) (Figures 2E and 2F; n ≥ 13 cells from each of 8 seedlings), resulting in reduction in cell sizes on the outer side in PMEI5oe at 0–400 μm from SAM compared with WT (average cell length on outer side 38.2 μm ± 2.6 in PMEI5oe compared with 57.2 μm ± 10.2 in WT) upon completion of hook formation (Figures 2G and S2B). Nevertheless, PMEI5oe and WT cells on the inner side of the hook did not markedly differ in terms of elongation rates (2.2% h^{-1} ± 0.9% in PMEI5oe compared with 2.4% h^{-1} ± 0.8% in WT) (Figures 2E and 2F). Altogether these data suggest that differential cell elongation relies on HG methylesterification and resulting increased wall stiffness on the inner side of apical hook in the WT. We then analyzed how the attenuation of HG methylesterification asymmetry influences hook development. Whereas WT seedlings formed a 180° bend, PMEI5oe seedlings could only bend to 135° and opened prematurely relative to WT seedlings (Figure 2H). These results indicate that asymmetric HG methylesterification contributes to differences in cell wall mechanical properties required for the differential cell elongation observed during hook development.

As apical hook development is a critical phase of seedling establishment, we investigated whether HG methylesterification changes affect seedling emergence, with WT and PMEI5oe seeds sown either on the soil surface or 5 mm underneath the soil. While both WT and PMEI5oe seedlings emerged when germinated on the soil surface, PMEI5oe seedlings failed to emerge from seeds that had been buried in the soil (Figures 2I–2K; n = 30 seeds, repeated 3 times). These data indicate that asymmetric HG methylesterification is crucial to proper apical hook development, and perturbing this asymmetry leads to hook developmental defects, which further impacts seedling emergence.

Auxin promotes HG methylesterification to mediate cell-wall composition asymmetry during hook development

The finding that asymmetric HG methylesterification is important for the differential growth observed during hook development prompted us to investigate which factors mediate this asymmetry. The domains of high HG methylesterification and auxin response overlap spatially during hook development and previously, exogenous auxin application has been shown to affect HG methylesterification during organ initiation in *Arabidopsis*.[12] Therefore, we analyzed whether auxin mediates differential HG methylesterification in the hook. We used a genetic approach to investigate the role of auxin in HG methylesterification. More specifically, we examined HG methylesterification in *yuc1D* mutants—which show enhanced auxin levels due to increased expression of YUCCA1, a rate-limiting enzyme in the indole-3-pyruvate pathway of auxin biosynthesis.[24] *yuc1D* seedlings displayed an over 2-fold and a 4-fold increase in HG methylesterification on the inner and outer sides, respectively, relative to WT seedlings (in *yuc1D*, LM20/LM19 ratio: 3.7 ± 1.7 on outer side and 4.3 ± 1.1 on inner side, compared to WT: 0.8 ± 0.1 on outer side and 1.9 ± 1.0 on inner side), which severely attenuated HG methylesterification asymmetry (Figures 3A and S3A; n ≥ 10 cells from each of 6 seedlings). Thus, the enhanced HG methylesterification observed in *yuc1D* seedlings phenocopied PMEI5oe seedlings. Conversely, suppressing auxin response by expression of dominant-negative *tir1E12K-GUS (tir1E12K)*[28] resulted in an almost 2-fold reduction in HG methylesterification

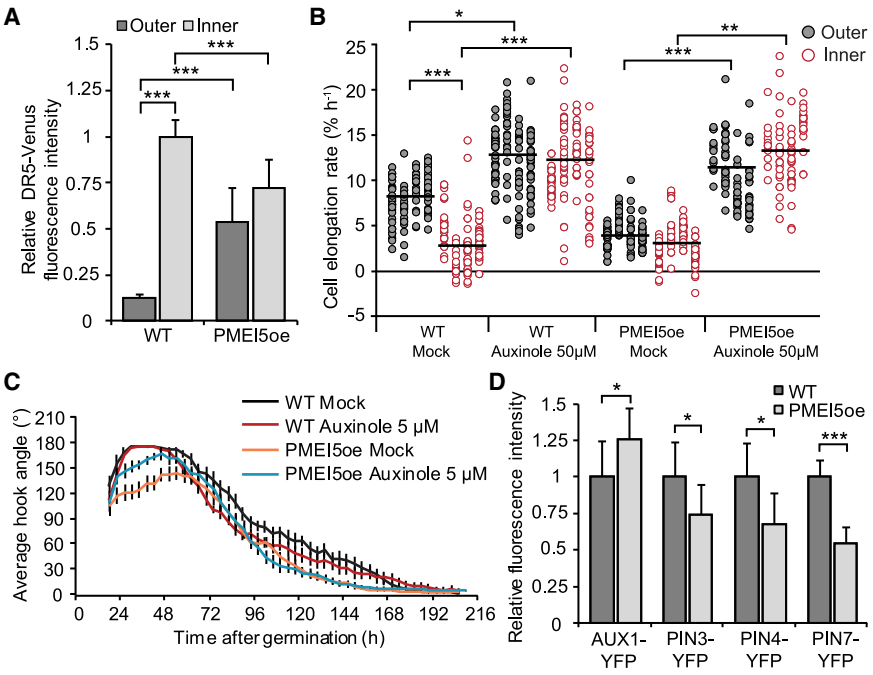

Figure 4. HG methylesterification affects auxin response

(A) Average nuclear DR5-Venus intensity on inner and outer sides of the hook in WT and PMEI5oe seedlings. n ≥ 11 cells from each of inner and outer side of 9 seedlings.

(B) Individual cell-elongation rates (% h^{-1}) at 0–400 μm upon 3 h mock and 50 μM auxinole treatment in WT and PMEI5oe seedlings. n ≥ 11 cells from each of 8 seedlings. Cells from individual seedlings are grouped vertically. Black horizontal lines indicate the mean.

(C) Apical hook development in WT and PMEI5oe upon mock and 5 μM auxinole treatment. n ≥ 12 seedlings.

(D) Quantification of PM signal of AUX1-YFP, PIN3-GFP, PIN4-GFP, and PIN7-GFP in epidermal cells at 0–400 μm from SAM during hook formation. For AUX1-YFP and PIN3-GFP, n = 5 cells from each of 10 seedlings. For PIN4-GFP and PIN7-GFP, n = 5 cells each of 9 seedlings. Statistical significance was determined by paired, two-tailed Student's t test, where *p < 0.05, **p < 0.005, ***p < 0.0005.

For (A), (B), and (D), error bars represent standard deviation of the mean. For (C), error bars represent standard error of the mean. See also Figure S4.

levels on the inner side of the hook compared to WT seedlings (on inner side, LM20/LM19 ratio in *tirE12K* 1.0 ± 0.1, compared to WT with 1.7 ± 0.2), while outer side HG methylesterification levels in *tirE12K* did not differ from WT (on outer side LM20/LM19 ratio in *tirE12K* 1.0 ± 0.1, compared to WT 0.9 ± 0.1) (Figures 3B and S3B; n ≥ 6 cells from each of 4 seedlings). We then examined cell elongation rates in *yuc1D* and *tirE12K* mutants. Compared with WT, *yuc1D* seedlings exhibited a markedly decreased cell elongation rate on the outer side of the hook (3.7% h^{-1} ± 1.2% in *yuc1D* compared to 6.6% h^{-1} ± 1.3% in WT), while cell elongation rates on the inner side did not differ significantly between *yuc1D* and WT (2.9% h^{-1} ± 0.9% in *yuc1D* compared to 3.6% h^{-1} ± 1.2% in WT) (Figures 3C and S3C; n ≥ 10 cells from each of 8 seedlings). Conversely, *tirE12K* seedlings exhibited elevated cell elongation rates on the inner side compared to WT (5.2% h^{-1} ± 1.7% compared to 3.6% h^{-1} ± 1.2% in WT), while the elongation rate of cells on the outer side did not differ significantly between *tirE12K* and WT (5.2% h^{-1} ± 0.6% in *tirE12K* compared to 6.6% h^{-1} ± 1.3% in WT) (Figures 3C and S3C; n ≥ 10 cells from each of 8 seedlings). Taken together, the enhanced HG methylesterification in *yuc1D* mutants and the converse in *tir1E12K* mutants, the resultant alterations in elongation rates, together with the spatial correlation between high auxin response and HG methylesterification in WT seedlings, suggest that auxin levels are positively associated with HG methylesterification.

HG methylesterification feeds back onto auxin response

Cell wall composition can impact the auxin response domain during hook development. For example, reduced xyloglucan levels attenuates the auxin response domain on the inner side of the hook and adversely affects hook development.[22] These observations, along with defects in hook development in PMEI5oe seedlings, prompted us to investigate whether HG methylesterification impacts the auxin response. Whereas high auxin response domain is restricted to the inner side of the hook in WT seedlings, PMEI5oe seedlings exhibited a broad auxin response domain that extended along both sides of the hook, increasing DR5 intensity on the outer side more than 4-fold (in PMEI5oe, outer DR5-Venus relative intensity 0.53 ± 0.18 compared with WT 0.12 ± 0.02). Thus, the loss of asymmetric HG methylesterification also perturbs auxin response domain asymmetry (Figures 4A and S4A; n ≥ 11 cells from each of inner and outer side of 9 seedlings). These results suggest a positive feedback loop between auxin and HG methylesterification during apical hook development.

Attenuation of auxin response rescues hook defects from enhanced HG methylesterification

The perturbation of asymmetric HG methylesterification in PMEI5oe seedlings negatively affects the differential growth necessary for hook formation. Interestingly, PMEI5oe seedlings display a broader auxin response domain than WT seedlings. We reasoned that this enhanced auxin response on the outer side in PMEI5oe (in contrast to WT) may repress cell elongation on this side, thereby attenuating differential growth across the hypocotyl. We addressed this hypothesis by suppressing the auxin response in PMEI5oe seedlings via auxinole treatment. Cell elongation rates were strongly enhanced by short-term auxinole application (50 μM over 3 h) to PMEI5oe seedlings relative to mock-treated control (upon auxinole 10.9% h^{-1} ± 2.3% and 13.8% h^{-1} ± 1.9% on outer and inner sides, respectively, compared to 4.3% h^{-1} ± 1.0% and 3.3% h^{-1} ± 1.6% on outer and inner sides upon mock treatment) with the elongation rates reaching levels similar to what was observed for auxinole-treated WT seedlings (12.6% h^{-1} ± 2.0% and 11.7% h^{-1} ± 2.2% on outer and inner sides, respectively) (Figures 4B and S4B; n ≥ 11 cells from each of 8 seedlings), causing hook development disruption

(Figure S4C). Moreover, when grown on medium supplemented with 5 μM auxinole (that did not affect WT), hook formation defects were partially rescued in PMEI5oe seedlings, with PMEI5oe seedlings reaching an average angle of 163° upon auxinole treatment compared with 132° upon mock treatment (Figure 4C; n ≥ 12 seedlings).

HG methylesterification mediates control of asymmetric auxin response via polar auxin transport

The asymmetric auxin response witnessed during hook development is established through the concerted action of the auxin transport machinery.[6,29] Therefore, we examined the behavior of specific auxin influx and efflux transporters to determine whether the broad auxin response domain in PMEI5oe seedlings was caused by perturbations in the auxin transport machinery. We observed a 25% increase in fluorescence levels for the auxin influx carrier AUX1-YFP at the plasma membrane (PM) in PMEI5oe seedlings relative to WT seedlings (Figures 4D and S4D). In contrast, the fluorescence signal for the auxin efflux carrier PIN1-GFP was absent from the PM, almost exclusively localized to intracellular structures in PMEI5oe seedlings. In comparison, the PIN1-GFP signal was localized to the PM of cells on the inner side of the hook in WT seedlings. Furthermore, in PMEI5oe seedlings, PM intensity of efflux carriers PIN3-GFP, PIN4-GFP, and PIN7-GFP were reduced to 74%, 67%, and 55% of WT levels, respectively (Figures 4E and S4D, for AUX1-YFP and PIN3-GFP, n = 10 cells from each of 10 seedlings, for PIN1-GFP, n ≥ 8 seedlings, for PIN4-GFP and PIN7-GFP, n = 5 cells from each of 9 seedlings). These results suggest that alterations in HG methylesterification could impact the polar auxin transport machinery and broaden the auxin response domain. Hence, our results suggest that, while auxin levels affect HG methylesterification, this methylesterification can also influence factors that drive auxin distribution patterns. Such a positive feedback loop would promote hypocotyl bending during apical hook formation.

DISCUSSION

Apical hook development is crucial to the survival and establishment of germinating seedlings, as it protects the fragile shoot apical meristem from the soil interface. Here, we show that differential growth during hook formation is mediated by a HG methylesterification gradient that depends on auxin distribution. Moreover, we discovered that HG methylesterification affects the transport machinery that controls auxin distribution in the hook. Our results thus reveal that tissue bending during hook formation is regulated by a positive mechanochemical feedback loop.

Auxin mediates differential cell elongation by influencing cell-wall stiffness

Several studies had previously demonstrated that the asymmetric auxin response across the hypocotyl is essential for proper hook development.[6,30] Auxin can either promote or repress cell elongation. Based on our data, the high auxin levels on the inner side, when compared to low levels on the outer side, repress cell elongation during apical hook formation. Nevertheless, how this asymmetric auxin response translates into differential cell elongation remains poorly understood. Interestingly, the auxin response domain spatially overlaps with pronounced differences in cell wall mechanical properties and reduced cell elongation on the inner side. Therefore, it is plausible that the auxin repression of cell elongation may be mediated via modulation of cell wall mechanics. Notably, exogenous IAA application can reduce cell elongation on the outer side, which usually shows low auxin response (Figures 1A–1E). Conversely, suppressing auxin response through auxinole application enhances elongation on the inner side of the hook (Figures 1F–1J). Hence, auxin can influence cell wall mechanical properties, as increased auxin levels correspond with significant differences in cell-wall properties and elongation, on the outer side of the hook (Figures 1K–1L and 1N), and the converse on the inner side of the hook upon auxin inhibition (Figures 1K, 1M, and 1N) These data suggest that the auxin-mediated modulation of cell wall mechanical properties may regulate differential cell elongation. Importantly, our results highlight that auxin effects on cell elongation are presumably concentration and context dependent and provide a plausible mechanism for organizing tissue-scale control of differential growth and mechanical properties via asymmetric distribution of auxin.

Our data suggest that asymmetric auxin distribution establishes differential cell elongation regions by affecting mechanical properties, and more specifically, wall stiffness. However, the pathways through which auxin alters mechanical properties in the apical hook have remained unknown. Furthermore, the link through which asymmetric auxin distribution translates to differences in mechanical properties and elongation rates across the hypocotyl remains unclear. Several recent studies have suggested that HG methylesterification influences wall structure, mechanical properties, growth anisotropy, and tissue patterning.[18,19,31] Our analysis of HG methylesterification showed that the inner side of the hook—characterized by low cell elongation and elasticity—exhibited longitudinal walls with highly methylesterified HG relative to the outer side (Figure 2A). Moreover, we found the perturbation of HG methylesterification asymmetry to severely affect mechanical properties (Figures 2B–2D) and differential cell elongation (Figures 2E and 2F), which resulted in defective hook formation (Figure 2H). Our results thus highlight the importance of mechanochemical asymmetry of the cell wall across the hypocotyl during hook formation.

Auxin response maxima and lower rates of cell elongation overlap with regions of high HG methylesterification in the hook. Furthermore, increased auxin levels (*yuc1D* mutant) and a suppressed auxin response (*tir1E12K*) showed opposite effects on HG methylesterification (Figures 3A and 3B), suggesting that asymmetric auxin distribution is linked to HG methylesterification. Thus, the auxin-mediated gradient in HG methylesterification could regulate the differential mechanical properties that are critical for the tissue-level differences in cell elongation that induce hypocotyl bending. Currently, the mechanism underlying auxin-promoted HG methylesterification remains unclear. Auxin is known to positively regulate the expression of several PMEIs,[32,33] although post-transcriptional mechanisms may also be involved in HG methylesterification. For example, auxin can alter apoplastic pH by activating PM-localized proton pumps,[13,34] which may modulate the activity of several wall-modifying enzymes that can subsequently affect HG

methylesterification. Intriguingly, cell wall sensors such as FERONIA have been shown to bind pectin[35] and also mediate in auxin response and pH changes[13,36] and thus could provide a link between auxin and cell wall compositional changes critical for differential growth. The plethora of PME and PMEI genes in *Arabidopsis*, assumptions of genetic redundancy, and the paucity of knowledge regarding their enzymatic properties all make it difficult to pinpoint the exact mechanism for how auxin mediates HG methylesterification, although immunohistochemical and genetic data clearly indicate a link between auxin and HG methylesterification with high auxin correlating with methylesterified HG. Previously, a link between auxin and HG methylesterification has been suggested during auxin-mediated organ initiation at the SAM.[18] For example, exogenous auxin application results in increase in de-methylesterified HG during organ initiation. In contrast, our results show that during hook development, high auxin levels on the inner side favor high methylesterified HG. These differential effects of auxin on HG methylesterification could reflect the different roles of auxin in organ initiation and differential growth. Whereas during organ initiation, auxin promotes tissue softening by favoring de-methylesterification, whereas, during hook development, high auxin levels on inner side restrict growth by mediating high methylesterification relative to outer side in the hook.

Cell-wall properties influence the auxin response domain in the apical hook

Intriguingly, PMEI5oe seedlings exhibited a strongly altered auxin response domain. In contrast with the WT seedlings—in which the auxin response was distinctly localized to the inner side—PMEI5oe seedlings exhibited significant DR5 expression in cells on the outer side as well (Figures 4A and S4A). AUX/LAX and PIN family proteins, which mediate polar auxin transport, have been shown to establish the asymmetric auxin response domain. Our data from PMEI5oe seedlings reveal alterations in the abundance of auxin transporters (AUX1, PIN1, PIN3, PIN4, and PIN7) in the PM, which could disrupt polar auxin transport (Figures 4E and S4C). Thus, a wider auxin response domain is most likely a consequence of the perturbed polar auxin transport associated with enhanced HG methylesterification that impacts both influx and efflux carriers at the PM. Previously, enhancing HG methylesterification was shown to cause altered PIN1 polarity that is critical for organ initiation. Whereas *pin1* mutant exhibits only minor defects in hook, PIN3, PIN4, and PIN7 play critical roles in hook development: the *pin3 pin4* as well as *pin4 pin7* double mutants exhibit severe hook defects.[6] Importantly, the levels of PIN3, PIN4 and PIN7 are all significantly reduced at the PM in PMEI5oe. Thus, our data now connect HG methylesterification with abundance of PIN3, PIN4 and PIN7 proteins that are critical during hook development.

There are two plausible routes through which changes in HG methylesterification affect the polar auxin transport machinery. First, an increase in HG methylesterification stimulates ectopic brassinosteroid (BR) signaling.[27] BR has been shown to stimulate PIN expression in shoots and to enhance PIN protein sorting at the PM.[37,38] However, our data show that enhanced HG methylesterification had an opposite effect on PIN levels at the PM. Alternatively, HG methylesterification can cause changes in cell wall mechanical properties that influence PIN PM levels as has been shown for PIN1.[39,40] While we cannot exclude the role of altered BR response, our data support that changes in cell wall mechanical properties influence the PM levels of auxin transporters.

Importantly, our data showing the effect of altering HG methylesterification on auxin response domain are indicative of a potential feedback whereby changes in cell wall composition may modulate auxin distribution to alter growth patterns. Intriguingly, changes in cell wall composition can significantly affect the polar auxin transport machinery. For example, the loss of xyloglucan in *xxt1 xxt2* mutant perturbed polar auxin transport machinery,[22] similar to what was observed in PMEI5oe seedlings with increased HG methylesterification. However, the effect of altered HG methylesterification on polar auxin transport is distinct from defects in the *xxt1 xxt2* mutant. For example, PIN1 was transcriptionally upregulated in xyloglucan mutants, whereas PIN1 was excluded from the PM and instead localized intracellularly in PME15oe seedlings. Hence, qualitative changes in cell wall composition can have distinct effects on the components of polar auxin transport machinery.

Based on our results, we suggest the following model for hook development. Local auxin response maxima favor a high degree of HG methylesterification on the inner side of the hypocotyl relative to the outer side (Figure 5). Peaucelle et al.[18] have shown that high HG methylesterification results in stiffer cell walls. Our results in the hook are consistent with this finding: our cell deformation assays indicate low and high deformation on the inner and outer side that overlap these differential HG methylesterification patterns. Thus, high HG methylesterification on the inner side of the hook results in stiffer walls on the inner side and asymmetric cell pliancy across the hypocotyl. In other words, spatial differences in wall mechanical properties translate into differential growth rates, which lead to hypocotyl bending. Enhanced HG methylesterification interferes with the auxin response pattern across the hypocotyl and perturbs spatial control of mechanical asymmetry, with increased auxin inhibiting growth on the outer side and resulting in defective hook development. We thus propose that HG methylesterification plays an instructive role on auxin pattern in a positive feedback loop, to amplify the asymmetry and further promote tissue bending. In support of this, we observed that the attenuation of auxin response by auxinole treatment largely mitigated the repressed cell elongation caused by PMEI5 overexpression (Figure 4B) and, furthermore, could reverse the defective hook development observed in PMEI5oe seedlings (Figure 4C). These results extend the finding in the shoot apical meristem, linking auxin to PME activity. However, whereas in meristem, auxin-mediated wall softening, results in promotion of cell elongation and organ outgrowth:[12] we show here that auxin can also repress cell elongation, through induced wall stiffening and HG methylesterification, leading to tissue bending.

Hook formation requires the dynamic control of spatial cell elongation gradients. Previous research has suggested that feedback loops between tissue mechanics and auxin distribution could enable continuous fine-tuning of growth, e.g., cell wall strain patterns instruct the polarity and abundance of PIN1 protein at the PM in the apical meristem.[39,40] During organ

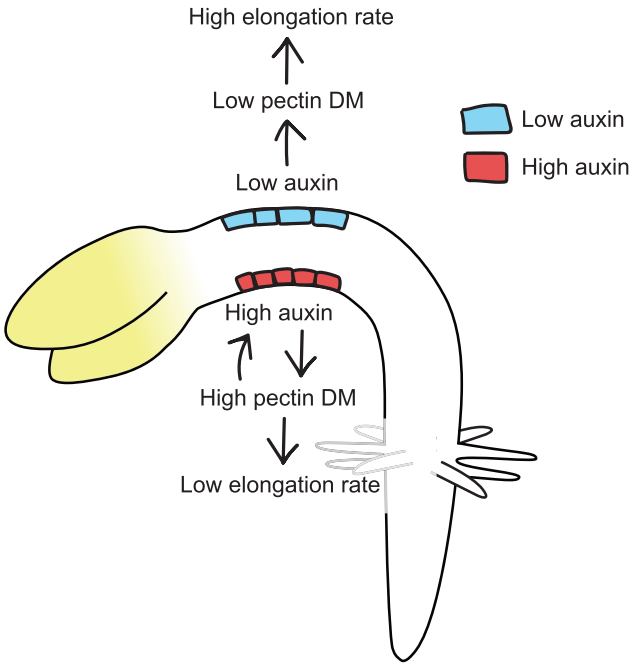

Figure 5. A schematic model of mechanochemical feedback during hook formation

During hook formation, auxin maxima is generated on the inner side by polar auxin transport. High auxin levels on inner side promote pectin with high degree of methylesterification (DM), stiffening the wall. Elevated DM pectin positively feeds back into the auxin machinery, reinforcing the auxin maximum on the inner side. High auxin and DM pectin result in a slower rate of cell elongation. Concurrently, low auxin levels on the outer side favor pectin demethylesterification and less wall stiffness, resulting in faster cell elongation on the outer side. The differences in cell elongation on two sides of the hypocotyl result in hypocotyl bending.

initiation, a feedback loop involves auxin-mediated tissue softening that feeds back into PIN1 polarity to coordinate local accumulation of auxin with organ outgrowth. In contrast, our data reveal asymmetric auxin distribution mediates tissue-level differential ratio of methylesterified to demethylestrified HG. The resulting spatial differences in mechanical properties with a rigid inner and relatively softer outer side in turn act on auxin transport machinery components PIN3, PIN4, PIN7, and AUX1 that are known to play a key role in hook development, to generate distinct domains of cell elongation to achieve bending. Hence, auxin distribution dynamically responds to asymmetries in mechanical properties to reinforce growth patterns. Thus, it is conceivable that asymmetric auxin distribution and cell wall composition result from interdependent mechanisms in which feedback between mechanochemical and hormonal signals reinforces growth asymmetry. Such interaction may reflect a general mechanism that operates also during apical hook formation as suggested by our results.

STAR★METHODS

Detailed methods are provided in the online version of this paper and include the following:

SUPPLEMENTAL INFORMATION

Supplemental Information can be found online at https://doi.org/10.1016/j.cub.2020.12.016.

ACKNOWLEDGMENTS

The authors thank Herman Höfte, Siobhan Braybrook, Alexis Peaucelle, and Anirban Baral for helpful discussions and comments on the manuscript. This work was funded by grants from Knut and Alice Wallenberg Foundation (2014-0032) and Vetenskapsrådet (2016-00504) to R.P.B.; R.S.L. was funded by a postdoctoral fellowship from the Kempe foundation to R.P.B. and O.H.; A.-L.R.-K. and D.K. labs are funded by Discovery Grants RGPIN-2018-05762 and RGPIN-2018-04897 from Natural Sciences and Engineering Research Council of Canada. The authors acknowledge the facilities and technical assistance of the Umeå Core Facility Electron Microscopy (UCEM) at the Chemical Biological Centre (KBC), Umeå University, a part of the National Microscopy Infrastructure NMI (VR-RFI 2016-00968).

AUTHOR CONTRIBUTIONS

K.J. and R.P.B. designed research; K.J., R.S.L., and D.K. performed research; K.J., R.S.L., D.K., A.-L.R-K., O.H., and R.P.B. analyzed data; K.J., D.K., A.-L.R-K., O.H., and R.P.B. wrote the paper.

DECLARATION OF INTERESTS

The authors declare no competing interests.

Received: September 11, 2020
Revised: November 17, 2020
Accepted: December 14, 2020
Published: January 7, 2021

REFERENCES

1. Raz, V., and Ecker, J.R. (1999). Regulation of differential growth in the apical hook of Arabidopsis. Development *126*, 3661–3668.
2. Mazzella, M.A., Casal, J.J., Muschietti, J.P., and Fox, A.R. (2014). Hormonal networks involved in apical hook development in darkness and their response to light. Front. Plant Sci. *5*, 52.
3. Friml, J., Wiśniewska, J., Benková, E., Mendgen, K., and Palme, K. (2002). Lateral relocation of auxin efflux regulator PIN3 mediates tropism in Arabidopsis. Nature *415*, 806–809.

4. Thimann, K.V. (1939). Auxins and the inhibition of plant growth. Biol. Rev. Camb. Philos. Soc. *14*, 314–337.

5. Schwark, A., and Schierle, J. (1992). Interaction of ethylene and auxin in the regulation of hook growth 0.1. The role of auxin in different growing regions of the hypocotyl hook of phaseolus-vulgaris. J. Plant Physiol. *140*, 562–570.

6. Zádníková, P., Petrásek, J., Marhavy, P., Raz, V., Vandenbussche, F., Ding, Z., Schwarzerová, K., Morita, M.T., Tasaka, M., Hejátko, J., et al. (2010). Role of PIN-mediated auxin efflux in apical hook development of Arabidopsis thaliana. Development *137*, 607–617.

7. Boerjan, W., Cervera, M.T., Delarue, M., Beeckman, T., Dewitte, W., Bellini, C., Caboche, M., Van Onckelen, H., Van Montagu, M., and Inzé, D. (1995). Superroot, a recessive mutation in Arabidopsis, confers auxin overproduction. Plant Cell *7*, 1405–1419.

8. Harper, R.M., Stowe-Evans, E.L., Luesse, D.R., Muto, H., Tatematsu, K., Watahiki, M.K., Yamamoto, K., and Liscum, E. (2000). The NPH4 locus encodes the auxin response factor ARF7, a conditional regulator of differential growth in aerial Arabidopsis tissue. Plant Cell *12*, 757–770.

9. Kierzkowski, D., and Routier-Kierzkowska, A.L. (2019). Cellular basis of growth in plants: geometry matters. Curr. Opin. Plant Biol. *47*, 56–63.

10. Majda, M., and Robert, S. (2018). The role of auxin in cell wall expansion. Int. J. Mol. Sci. *19*, 951.

11. Nemhauser, J.L., Hong, F., and Chory, J. (2006). Different plant hormones regulate similar processes through largely nonoverlapping transcriptional responses. Cell *126*, 467–475.

12. Braybrook, S.A., and Peaucelle, A. (2013). Mechano-chemical aspects of organ formation in Arabidopsis thaliana: the relationship between auxin and pectin. PLoS ONE *8*, e57813.

13. Barbez, E., Dünser, K., Gaidora, A., Lendl, T., and Busch, W. (2017). Auxin steers root cell expansion via apoplastic pH regulation in *Arabidopsis thaliana*. Proc. Natl. Acad. Sci. USA *114*, E4884–E4893.

14. Zablackis, E., Huang, J., Müller, B., Darvill, A.G., and Albersheim, P. (1995). Characterization of the cell-wall polysaccharides of Arabidopsis thaliana leaves. Plant Physiol. *107*, 1129–1138.

15. Sterling, J.D., Quigley, H.F., Orellana, A., and Mohnen, D. (2001). The catalytic site of the pectin biosynthetic enzyme alpha-1,4-galacturonosyltransferase is located in the lumen of the Golgi. Plant Physiol. *127*, 360–371.

16. Wolf, S., Mouille, G., and Pelloux, J. (2009). Homogalacturonan methylesterification and plant development. Mol. Plant *2*, 851–860.

17. Jolie, R.P., Duvetter, T., Van Loey, A.M., and Hendrickx, M.E. (2010). Pectin methylesterase and its proteinaceous inhibitor: a review. Carbohydr. Res. *345*, 2583–2595.

18. Peaucelle, A., Braybrook, S.A., Le Guillou, L., Bron, E., Kuhlemeier, C., and Höfte, H. (2011). Pectin-induced changes in cell wall mechanics underlie organ initiation in Arabidopsis. Curr. Biol. *21*, 1720–1726.

19. Peaucelle, A., Wightman, R., and Höfte, H. (2015). The control of growth symmetry breaking in the Arabidopsis hypocotyl. Curr. Biol. *25*, 1746–1752.

20. Bou Daher, F., Chen, Y., Bozorg, B., Clough, J., Jönsson, H., and Braybrook, S.A. (2018). Anisotropic growth is achieved through the additive mechanical effect of material anisotropy and elastic asymmetry. eLife *7*, e38161.

21. Peaucelle, A., Louvet, R., Johansen, J.N., Höfte, H., Laufs, P., Pelloux, J., and Mouille, G. (2008). Arabidopsis phyllotaxis is controlled by the methylesterification status of cell-wall pectins. Curr. Biol. *18*, 1943–1948.

22. Aryal, B., Jonsson, K., Baral, A., Sancho-Andres, G., Routier-Kierzkowska, A.L., Kierzkowski, D., and Bhalerao, R.P. (2020). Interplay between cell wall and auxin mediates the control of differential cell elongation during apical hook development. Curr. Biol. *30*, 1733–1739.

23. Silk, W.K., and Erickson, R.O. (1978). Kinematics of hypocotyl curvature. Am. J. Bot. *65*, 310–319.

24. Zhao, Y., Christensen, S.K., Fankhauser, C., Cashman, J.R., Cohen, J.D., Weigel, D., and Chory, J. (2001). A role for flavin monooxygenase-like enzymes in auxin biosynthesis. Science *291*, 306–309.

25. Weber, A., Braybrook, S., Huflejt, M., Mosca, G., Routier-Kierzkowska, A.L., and Smith, R.S. (2015). Measuring the mechanical properties of plant cells by combining micro-indentation with osmotic treatments. J. Exp. Bot. *66*, 3229–3241.

26. Kierzkowski, D., Nakayama, N., Routier-Kierzkowska, A.L., Weber, A., Bayer, E., Schorderet, M., Reinhardt, D., Kuhlemeier, C., and Smith, R.S. (2012). Elastic domains regulate growth and organogenesis in the plant shoot apical meristem. Science *335*, 1096–1099.

27. Wolf, S., Mravec, J., Greiner, S., Mouille, G., and Höfte, H. (2012). Plant cell wall homeostasis is mediated by brassinosteroid feedback signaling. Curr. Biol. *22*, 1732–1737.

28. Yu, H., Zhang, Y., Moss, B.L., Bargmann, B.O., Wang, R., Prigge, M., Nemhauser, J.L., and Estelle, M. (2015). Untethering the TIR1 auxin receptor from the SCF complex increases its stability and inhibits auxin response. Nat. Plants *1*, 1.

29. Vandenbussche, F., Petrásek, J., Zádníková, P., Hoyerová, K., Pesek, B., Raz, V., Swarup, R., Bennett, M., Zazímalová, E., Benková, E., and Van Der Straeten, D. (2010). The auxin influx carriers AUX1 and LAX3 are involved in auxin-ethylene interactions during apical hook development in Arabidopsis thaliana seedlings. Development *137*, 597–606.

30. Žádníková, P., Wabnik, K., Abuzeineh, A., Gallemi, M., Van Der Straeten, D., Smith, R.S., Inzé, D., Friml, J., Prusinkiewicz, P., and Benková, E. (2016). A model of differential growth-guided apical hook formation in plants. Plant Cell *28*, 2464–2477.

31. Haas, K.T., Wightman, R., Meyerowitz, E.M., and Peaucelle, A. (2020). Pectin homogalacturonan nanofilament expansion drives morphogenesis in plant epidermal cells. Science *367*, 1003–1007.

32. Chapman, E.J., Greenham, K., Castillejo, C., Sartor, R., Bialy, A., Sun, T.P., and Estelle, M. (2012). Hypocotyl transcriptome reveals auxin regulation of growth-promoting genes through GA-dependent and -independent pathways. PLoS ONE *7*, e36210.

33. Goda, H., Sawa, S., Asami, T., Fujioka, S., Shimada, Y., and Yoshida, S. (2004). Comprehensive comparison of auxin-regulated and brassinosteroid-regulated genes in Arabidopsis. Plant Physiol. *134*, 1555–1573.

34. Takahashi, K., Hayashi, K., and Kinoshita, T. (2012). Auxin activates the plasma membrane H+-ATPase by phosphorylation during hypocotyl elongation in Arabidopsis. Plant Physiol. *159*, 632–641.

35. Feng, W., Kita, D., Peaucelle, A., Cartwright, H.N., Doan, V., Duan, Q., Liu, M.C., Maman, J., Steinhorst, L., Schmitz-Thom, I., et al. (2018). The FERONIA receptor kinase maintains cell-wall integrity during salt stress through Ca^{2+} signaling. Curr. Biol. *28*, 666–675.e5.

36. Schoenaers, S., Balcerowicz, D., Breen, G., Hill, K., Zdanio, M., Mouille, G., Holman, T.J., Oh, J., Wilson, M.H., Nikonorova, N., et al. (2018). The auxin-regulated CrRLK1L kinase ERULUS controls cell wall composition during root hair tip growth. Curr. Biol. *28*, 722–732.e6.

37. Li, L., Xu, J., Xu, Z.H., and Xue, H.W. (2005). Brassinosteroids stimulate plant tropisms through modulation of polar auxin transport in Brassica and Arabidopsis. Plant Cell *17*, 2738–2753.

38. Retzer, K., Akhmanova, M., Konstantinova, N., Malínská, K., Leitner, J., Petrášek, J., and Luschnig, C. (2019). Brassinosteroid signaling delimits root gravitropism via sorting of the Arabidopsis PIN2 auxin transporter. Nat. Commun. *10*, 5516.

39. Heisler, M.G., Hamant, O., Krupinski, P., Uyttewaal, M., Ohno, C., Jönsson, H., Traas, J., and Meyerowitz, E.M. (2010). Alignment between PIN1 polarity and microtubule orientation in the shoot apical meristem reveals a tight coupling between morphogenesis and auxin transport. PLoS Biol. *8*, e1000516.

40. Nakayama, N., Smith, R.S., Mandel, T., Robinson, S., Kimura, S., Boudaoud, A., and Kuhlemeier, C. (2012). Mechanical regulation of auxin-mediated growth. Curr. Biol. *22*, 1468–1476.

41. Cutler, S.R., Ehrhardt, D.W., Griffitts, J.S., and Somerville, C.R. (2000). Random GFP:cDNA fusions enable visualization of subcellular structures in cells of Arabidopsis at a high frequency. Proc. Natl. Acad. Sci. USA *97*, 3718–3723.

42. Heisler, M.G., Ohno, C., Das, P., Sieber, P., Reddy, G.V., Long, J.A., and Meyerowitz, E.M. (2005). Patterns of auxin transport and gene expression during primordium development revealed by live imaging of the Arabidopsis inflorescence meristem. Curr. Biol. *15*, 1899–1911.

43. Belteton, S.A., Sawchuk, M.G., Donohoe, B.S., Scarpella, E., and Szymanski, D.B. (2018). Reassessing the roles of PIN proteins and anticlinal microtubules during pavement cell morphogenesis. Plant Physiol. *176*, 432–449.

44. Swarup, R., Kargul, J., Marchant, A., Zadik, D., Rahman, A., Mills, R., Yemm, A., May, S., Williams, L., Millner, P., et al. (2004). Structure-function analysis of the presumptive Arabidopsis auxin permease AUX1. Plant Cell *16*, 3069–3083.

45. Barbier de Reuille, P., Routier-Kierzkowska, A.L., Kierzkowski, D., Bassel, G.W., Schüpbach, T., Tauriello, G., Bajpai, N., Strauss, S., Weber, A., Kiss, A., et al. (2015). MorphoGraphX: a platform for quantifying morphogenesis in 4D. eLife *4*, 05864.

STAR★METHODS

KEY RESOURCES TABLE

REAGENT or RESOURCE	SOURCE	IDENTIFIER
Antibodies		
LM19 (Rat IgM)	Plantprobes	Cat. No. LM19; RRID: AB_2734788
LM20 (Rat IgM)	Plantprobes	Cat. No. LM20; RRID: AB_2734789
Cy5 anti-Rat (Rabbit IgG)	Jackson ImmunoResearch	RRID: AB_2338263
Biological Samples		
35S::PMEI5	[27]	N/A
yuc1D	[24]	N/A
pTIR1::tir1E12K-GUS	[28]	N/A
LTI6a-GFP	[41]	N/A
DR5::Venus	[42]	N/A
pPIN1::PIN1-GFP	[6]	N/A
pPIN3::PIN3-GFP	[6]	N/A
pPIN4::PIN4-GFP	[43]	N/A
pPIN7::PIN7-GFP	[43]	N/A
pAUX1::AUX-GFP	[44]	N/A
Chemicals, peptides, and recombinant proteins		
Murashige and Skoog (MS) medium	Duchefa	M0222
LR White Medium Grade	TAAB UK	L012
Indole-3-acetic acid (IAA)	Sigma-Aldrich	1003530010
Auxinole	MedChemExpress	HY-111444
Plant Agar	Duchefa Biochemie	P1001
MES hydrate	Sigma-Aldrich	M5287
Dimethyl sulfoxide (DMSO)	Sigma-Aldrich	D8418-500ML
Paraformaldehyde 16% (w/v)	ThermoFisher	28908
Experimental models: organisms/strains		
Arabidopsis thaliana	NASC	N1092
Software and algorithms		
Microsoft Excel (Office Professional Plus 2016)	Microsoft	N/A
ImageJ 1.50e	N/A	https://imagej.net/Fiji/Downloads

RESOURCE AVAILABILITY

Lead contact

Further information and requests for resources and reagents should be directed to and will be fulfilled by the Lead Contact, Rishikesh P. Bhalerao (rishi.bhalerao@slu.se).

Materials availability

This study has not generated any new reagents.

Data and code availability

This study did not generate any unique dataset or code.

EXPERIMENTAL MODEL AND SUBJECT DETAILS

Plant material

The *Arabidopsis thaliana* ecotype Columbia-0 wild-type and the following transgenic lines were used in this study: 35S::PMEI5 (PMEI5oe),[27] *yuc1D*,[24] *pTIR1::tir1E12K-GUS*,[28] LTI6a-GFP,[41] DR5::Venus.[42] pPIN1::PIN1-GFP, pPIN3::PIN3-GFP,[6] pPIN4::PIN4-GFP, pPIN7::PIN7-GFP,[43] pAUX1::AUX1-YFP[44]

Growth conditions

Plants were grown on square Petri dishes supplied with ¾ ¾ ¾ MS (2.2g/l Murashige & Skoog nutrient mix (Duchefa), 0.8% (w/v) plant agar (Duchefa), 0.5% (w/v) sucrose, 2.5mM 2-Morpholinoethanesulfonic acid (MES) (Sigma-Aldrich) buffered to pH 5.8 with KOH. For confocal microscopy and macro-confocal analysis, seeds were stratified for 2 days at 4°C, given a 6 hours light treatment and subsequently grown in darkness on vertically oriented agar Petri dishes at 21°C for the required time length. For time-lapse analysis of apical hook development, pharmacological treatment using auxinole (Hölzel Biotech), 5 μM auxinole dissolved in dimethyl sulfoxide (DMSO) (Sigma-Aldrich) from a stock solution of 50 mM auxinole was added to the medium, and the equivalent amount of solvent was added to the mock treatment.

METHOD DETAILS

Immunohistochemistry

Seedlings were fixed using 4% paraformaldehyde in PBS buffer for 45 minutes, and subsequently washed with PBS buffer 4 times. Samples were then sequentially dehydrated in 30 minute increments at 30%, 50%, 70%, 90% and 100% ethanol in PBS. LR White Medium grade (TAAB, UK) was added to samples dropwise to 10%, and incubated at 4°C for 6h. Solution was then exchanged for 50% LR White in PBS and incubated overnight at 4°C. Solution was then exchanged for 100% LR White in 3 sequential 12h incubations at 4°C. All LR White incubations were performed on a shaker table at 120 rpm. Samples were then cured at 60°C for 36 hours. Samples were sectioned at 2.5 μm thickness using a Reichert Ultracut S Wild M3Z microtome mounted with a Diatome Histo Diamond Knife (8.0mm 45° angle). Sections were placed on glass slides. Immunolabeling was performed on sections using antibodies with the following dilutions: Primary antibodies Rat-LM19 and Rat-LM20 (PlantProbes, UK) were diluted 1:50 with PBS buffer. Secondary antibody anti-Rat Cy5 (Jackson ImmunoResearch, UK) was diluted 1:200. Imaging was performed using a Carl Zeiss LSM780 using a 40x lens (Zeiss C-Apochromat 40x/1.2 W Corr M27). Cy5 was excited at 633 nm. Quantification of signal intensity of LM19 and LM20-labeled sections was performed on images acquired under strictly identical acquisition parameters (resolution, laser power, photomultiplier, offset and zoom factor). Sequential sections were labeled with LM19 and LM20 to enable dual labeling of the same cells. Ratio between LM19 and LM20 was obtained using ImageJ by drawing a 0.5 μm segmented line along outer longitudinal epidermal walls, and obtaining the average fluorescence intensity of that line. For analyzing HG methylesterification in the WT and investigating the effect of PMEI overexpression or enhancing auxin, WT, PMEI5oe and *yuc1-D* were analyzed together. To investigate effect of suppressing auxin response on HG methylesterification, WT and *tirE12K* were analyzed together in a separate experiment.

Time-lapse imaging of cell elongation

Seeds were given 6 h light treatment and subsequently grown on vertical agar Petri dishes in darkness and imaging was performed 16-20 h post-germination, corresponding to the hook formation phase. Seedlings were imaged on vertically oriented agar Petri dishes using a Nikon AZ-C2 vertical macro-confocal equipped with 5x/0.5 WD 15 mm macro-objective at 3-hour intervals in a dark room. Seedlings expressing LTI6a-GFP were excited at 488 nm and emission was detected using spectral detector. Between laser exposures, Petri dishes were wrapped in aluminum foil to minimize exposure to light. Under these conditions, hypocotyl elongation and hook development were not significantly different from dark-grown seedlings over the course of 24 hours subsequent to initial excitation. Cell elongation was measured using ImageJ, where cell length for each cell was measured at two time points, using the segmented line tool. From this, cell elongation percentage per hour was calculated. For pharmacological treatments using indole-3-acetic acid (IAA) or auxinole, seedlings were imaged and subsequently submerged in liquid ½ MS medium supplemented with 500 nM IAA (Sigma-Aldrich), or 50 μM auxinole. Auxinole was diluted from a 50 mM stock solution dissolved in DMSO, and IAA was diluted from a 500 μM stock solution dissolved in DMSO. Mock treatments were supplied with the equivalent amount of solvent. In order to investigate the effect of suppressing auxin response on growth, WT and PMEI5oe treated with auxinole (Figures 1F–1J, 4B, and S4B) were analyzed at the same time. For analysis of WT, *yuc1D* and *tirE12K,* not expressing a plasma-membrane marker, seedlings were incubated in darkness in liquid ½ MS medium supplemented with propidium iodide (10 mg/mL) for 1 h prior to imaging.

Cell length measurements

Seeds were grown on vertical agar Petri dishes in darkness and imaging was performed 24-28 h post-germination, corresponding to the early hook maintenance phase. Seedlings were imaged by confocal microscopy using a Carl Zeiss LSM780 equipped with a 25x lens (Zeiss Plan-Neofluar 25x/0.8 W Corr DIC M27). Cell lengths were obtained using ImageJ by drawing a segmented line along the length of each cell in the region of 0-400 μm from SAM.

Time-lapse analysis of apical hook development

For time-lapse analysis of apical hook development seedlings were grown vertically on Petri dishes in a dark room at 21°C illuminated only with far-infrared light source. Seedlings were photographed at 4h intervals using a Canon D50 camera without infrared filter. Hook curvature was measured using the angle tool in the software ImageJ, whereby the angle between the hypocotyl axis vector and cotyledons was measured (See Figure 2H inset). For each time-lapse analysis $n \geq 12$ seedlings per treatment. For all treatments, seedlings were germinated and grown on medium supplemented with the respective chemical dissolved in DMSO. Mock treatments were supplemented with an equivalent amount of DMSO.

Quantitative analysis of plasma membrane intensity

For analysis of AUX1-YFP, PIN3-GFP, PIN4-GFP and PIN7-GFP fluorescence intensity at the PM, confocal images were acquired using identical acquisition parameters (resolution, laser power, photomultiplier, offset and zoom factor) between WT and PMEI5oe seedlings. Intensity was measured by outlining the PM with a segmented line along the whole membrane and calculating the average intensity using ImageJ. For AUX1-YFP and PIN3-GFP 10 cells from each of 10 seedlings were analyzed. For PIN4-GFP and PIN7-GFP, 5 cells from each of 9 seedlings were analyzed.

Quantitative analysis of DR5::Venus intensity

Z stacks of seedlings expressing DR5::Venus were imaged by confocal microscopy under non-saturating imaging conditions, where identical acquisition parameters (resolution, laser power, photomultiplier, offset and zoom factor) were used between WT and PMEI5oe seedlings. Fluorescence signal between 0-400 μm from SAM was segmented longitudinally into a inner and outer dataset. For each dataset, the ImageJ plugin 3D Objects Counter was used to identify Venus-expressing objects (nuclei), and to obtain mean fluorescence intensity. For all sample analyses, identical threshold parameters (size and signal intensity) were used. For each genotype and dataset $\geq$15 cells from each of 9 seedlings were analyzed.

Analysis of cell deformation

Seedlings expressing PM marker LTI6a-GFP were first inflated by immersion in H_2O for 30 minutes. Subsequently Z stacks of seedlings were obtained by confocal microscopy. Following imaging, seedlings were then transferred to medium with 0.35 M NaCl for 30 minutes to deflate cells. Epidermal cell surface area from Z stacks was calculated using the software MorphographX as described previously.[26,45] The change in cell surface area from H_2O treatment to 0.35 M NaCl treatment was calculated using MorphographX. Heatmaps in Figures 1K–1M, 2B, and 2C were generated by averaging cell size change for each cell with its direct neighbors, to emphasize tissue-level patterns. Analysis of the elastic deformation in WT and the effect of altering HG methylesterification on elastic deformation was performed by comparing WT and PMEI5oe seedlings at the same time. The effect of auxin or suppressing auxin response on elastic deformation was performed in separate experiment by adding IAA and auxinole or mock treatments of WT.

Soil emergence assay

Sterilized seeds were stratified in sterile H_2O at 4°C for 2 days and subsequently pipetted onto the soil surface in pots. For germination inside soil, a 5 mm layer of soil was added on top of seeds. Pots were then placed in a growth chamber at 22°C with 16h light/8h dark cycle for 5 days. Seedlings emerging at the soil surface were then counted. For each treatment, 30 seeds per genotype were sown.

Definition of apical hook outer and inner side

Data obtained from confocal imaging of the hook was divided into four equally sized radial quadrants, the outer quadrant, two lateral quadrants and one inner quadrant. For comparison of cells on the outer versus inner side, we only considered data from the outer and inner quadrants, and disregarded the lateral quadrants.

QUANTIFICATION AND STATISTICAL ANALYSIS

Statistical significance was determined using Microsoft Excel, employing a paired, two-tailed Student's t test, on averages of biological replicates. For all analyses, *$p < 0.05$, **$p < 0.005$, ***$p < 0.0005$, as indicated in figures. Error bars in figures represent either standard deviation of the mean or standard error of the mean, as indicated in figure legends. Replicate numbers are indicated in figure legends.

Current Biology, Volume *31*

Supplemental Information

Mechanochemical feedback mediates tissue bending required for seedling emergence

Kristoffer Jonsson, Rahul S. Lathe, Daniel Kierzkowski, Anne-Lise Routier-Kierzkowska, Olivier Hamant, and Rishikesh P. Bhalerao

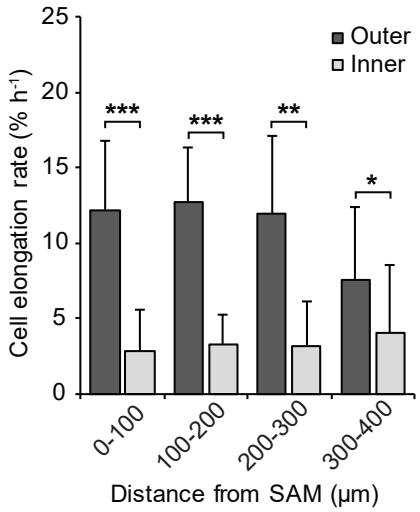

Figure S1. Cell elongation rates during hook formation, Related to Figure 1

Cell elongation rates (% h-1) during formation in WT, pooled into 100 µm longitudinal zones from the shoot apical meristem (SAM). n ≥ 18 cells per zone from each of 6 seedlings. Error bars represent standard deviation of the mean. Statistical significance was determined by paired, two-tailed student's t test, where *P < 0.05, **P < 0.005, ***P < 0.0005.

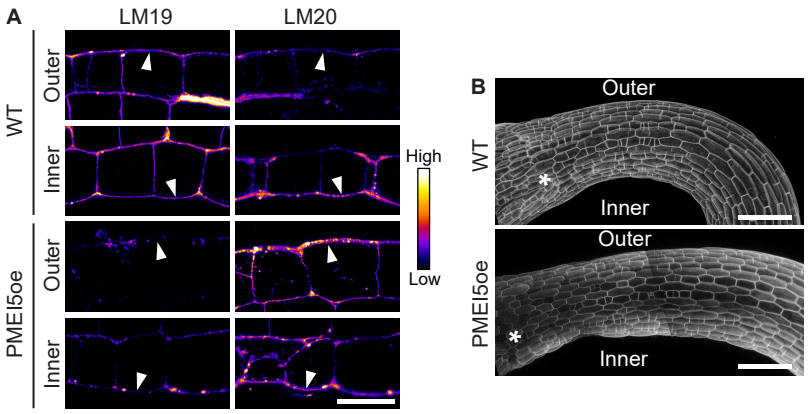

Figure S2. Pectin methylesterification and cell lengths in WT and PMEI5oe seedlings, Related to Figure 2

(A) Immunolabeling of longitudinal epidermal cell walls with LM19 and LM20, on the outer and inner side of WT and PMEI5oe seedlings during hook formation. White arrowheads indicate outer longitudinal walls. **(B)** Cell lengths in WT and PMEI5oe during early hook maintenance. White asterisks mark the position of SAM. Scale bars: in **A**, 10 µm; in **B**, 100 µm

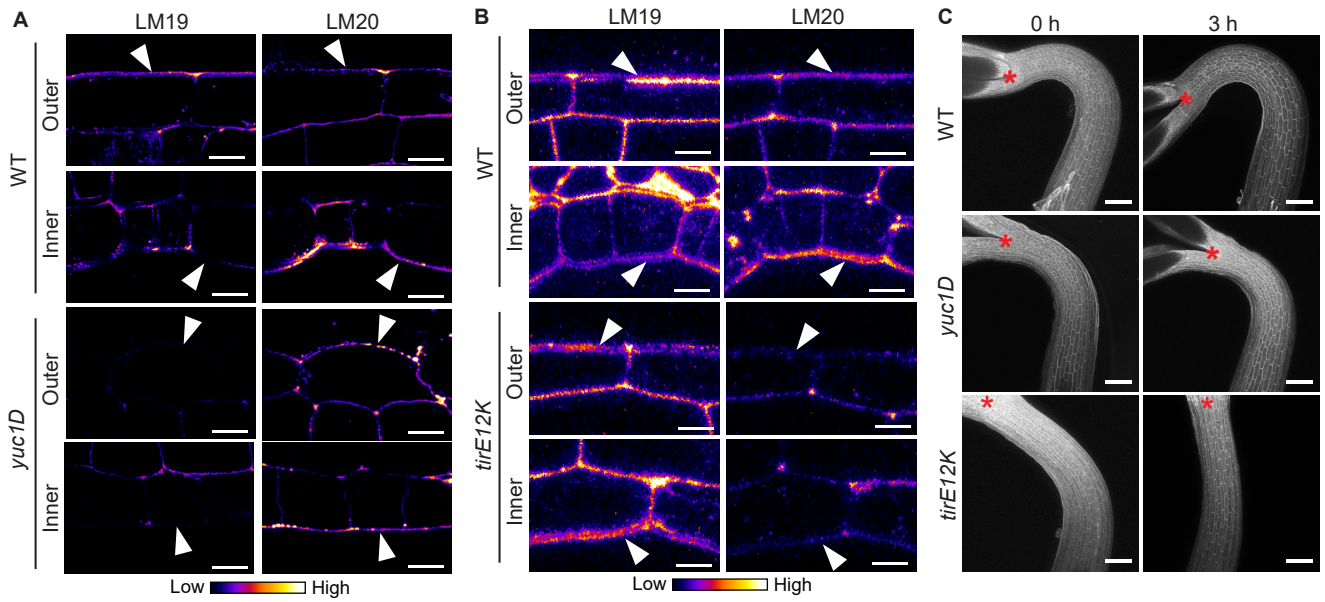

Figure S3. Auxin perturbation impacts pectin methylesterification and cell elongation, Related to Figure 3

(A-B) Immunolabeling of longitudinal epidermal cell walls with LM19 and LM20, on the outer and inner side of WT and *yuc1D* seedlings **(A)**, and WT and **tirE12K** seedlings **(B)** during hook formation. White arrowheads indicate outer longitudinal walls. **(C)** Macro-confocal time-lapse of cells in WT, *yuc1D* and *tirE12K* seedlings at 0 h and 3 h during formation. Red asterisks mark the position of SAM. Scale bars: in **A** and **B**, 10 µM; in **C**, 100 µm.

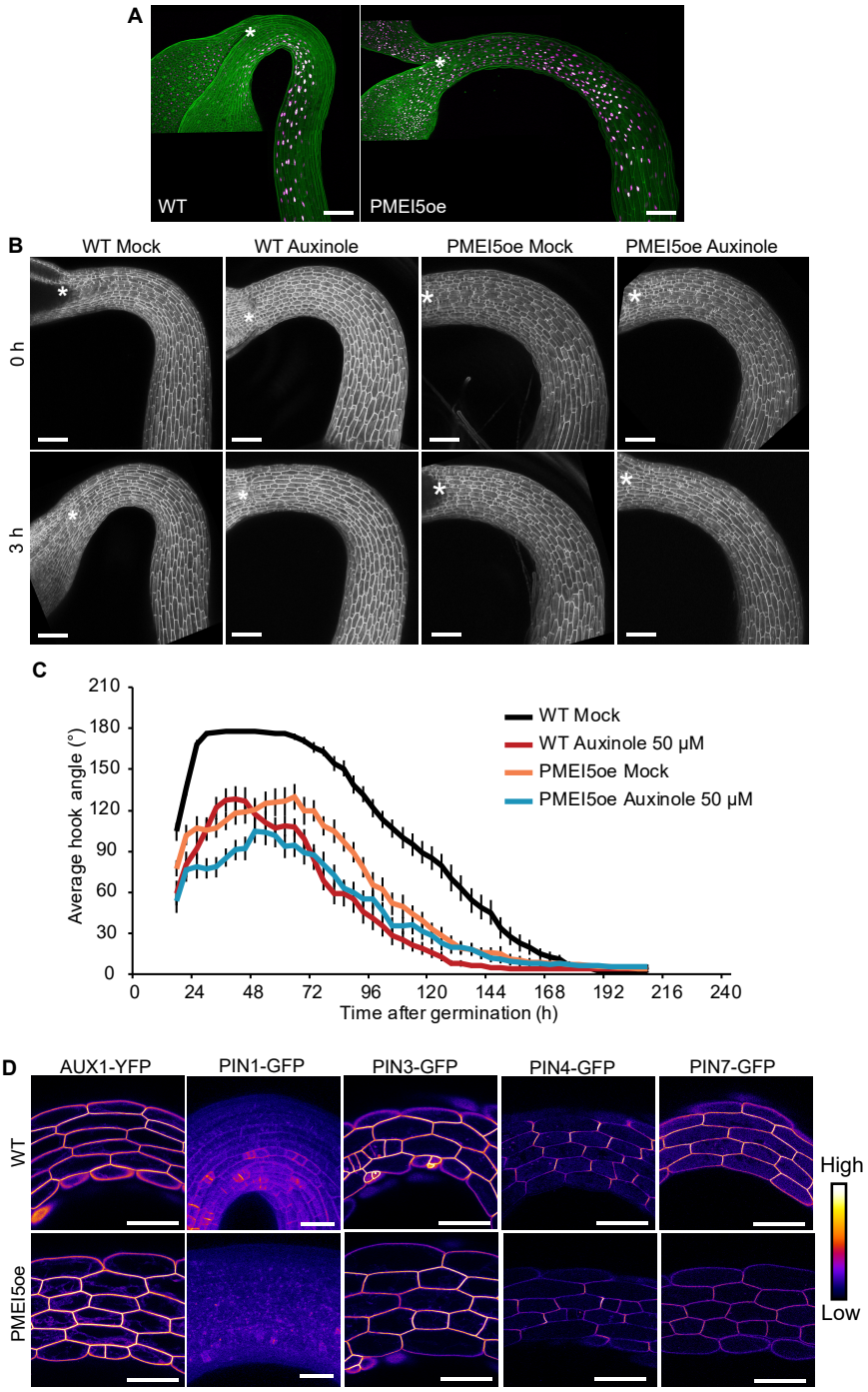

Figure S4. Interaction between pectin methylesterification, auxin response and polar auxin transport in control of differential growth, Related to Figure 4

(A) DR5-Venus expression (magenta) in WT and PMEI5oe seedlings. Cell periphery is counterstained with propidium iodide (green). **(B)** Macro-confocal time-lapse of cells in WT and PMEI5oe upon mock treatment and auxinole 50 µM treatment at 0 h and 3 h during formation. **(C)** Apical hook development in WT and PMEI5oe upon mock and 50 µM auxinole treatment. n = 16 seedlings. Error bars represent standard error of the mean. **(D)** PM fluorescence signal of AUX1-YFP, PIN1-GFP, PIN3-GFP, PIN4-GFP and PIN7-GFP in epidermal cells at 0-400 µm from SAM in WT and PMEI5oe seedlings during hook formation. White asterisks mark the position of SAM. Scale bars: In **A** and **B** 100µm; in **D** 50 µm.